

Unstable dimension variability, heterodimensional cycles, and blenders in the border-collision normal form.

P.A. Glendinning[†] and D.J.W. Simpson[‡]

[†]Department of Mathematics, University of Manchester, Manchester, UK

[‡]School of Mathematical and Computational Sciences, Massey University, Palmerston North, New Zealand

November 14, 2022

Abstract

Chaotic attractors commonly contain periodic solutions with unstable manifolds of different dimensions. This allows for a zoo of dynamical phenomena not possible for hyperbolic attractors. The purpose of this Letter is to demonstrate these phenomena in the border-collision normal form. This is a continuous, piecewise-linear family of maps that is physically relevant as it captures the dynamics created in border-collision bifurcations in diverse applications. Since the maps are piecewise-linear they are relatively amenable to an exact analysis and we are able to explicitly identify parameter values for heterodimensional cycles and blenders. For a one-parameter subfamily we identify bifurcations involved in a transition through unstable dimension variability. This is facilitated by being able to compute periodic solutions quickly and accurately, and the piecewise-linear form should provide a useful test-bed for further study.

1 Differing dimensions of instability

Chaotic attractors of one-dimensional non-invertible maps and two-dimensional invertible maps have one unstable direction locally. For higher dimensional maps the dimensions of the unstable manifolds of periodic orbits within a chaotic attractor can differ, and this can occur also for ODEs. This phenomenon is known as *unstable dimension variability* (UDV). It is expected to be common for chaotic attractors in mathematical models with sufficiently many variables [30, 38]. UDV implies the existence of orbits that spend arbitrarily long times close to an unstable manifold of one dimension, and arbitrarily long times close to an unstable manifold of another dimension [25, 8]. It follows that finite-time Lyapunov exponents fluctuate about zero as the system evolves [9, 37]. It further follows that numerical solutions may differ wildly from actual orbits. This lack of ‘shadowing’ is problematic for the applicability of a mathematical model [26, 13].

One mechanism that implies UDV is the existence of a *heterodimensional cycle* — a heteroclinic connection between saddle objects with unstable manifolds of different dimensions. If an attractor contains a heterodimensional cycle, then it has UDV [7]. A given heterodimensional cycle is at least codimension-one, and recent advances in numerical methods have led to the identification of heterodimensional cycles in an ODE model of intracellular calcium dynamics [40, 22].

A consequence of UDV is that the dimension of a stable or unstable manifold can appear to be greater than that of its local component. Such manifolds are termed *blenders* [5, 6]. Blenders form from heteroclinic cycles between invariant sets where at least one of these is chaotic and the existence of a heterodimensional cycle, and hence UDV, persists as parameters are varied. In such systems the codimension-one intersection between stable and unstable manifolds is made persistent if the m -dimensional invariant manifold of one of the sets aligns so that it has a projection that is effectively $(m + 1)$ -dimensional. Blenders in some ways generalise the Smale horseshoe to higher dimensions and provide a way to establish the robustness of properties relating to a lack of hyperbolicity [7]. Recently Hittmeyer *et. al.* [23, 24] numerically identified blenders in a smooth three-dimensional map.

2 The border-collision normal form

Border-collision bifurcations (BCBs) occur when a fixed point of a piecewise-smooth map collides with a boundary (switching manifold) where the functional form of the map changes. They have been identified as the onset of chaos and other dynamics in applications including power electronics [41, 34], mechanical systems with stick-slip friction [12, 36], and economics [29]. Near a BCB the dynamics are well-approximated by a piecewise-linear map [32]. The border-collision normal form (BCNF) then results from a change of coordinates [28, 11]. In two dimensions this form is

$$x \mapsto \begin{cases} A_L x + b, & x_1 \leq 0, \\ A_R x + b, & x_1 \geq 0, \end{cases} \quad (2.1)$$

where

$$A_L = \begin{bmatrix} \tau_L & 1 \\ -\delta_L & 0 \end{bmatrix}, \quad A_R = \begin{bmatrix} \tau_R & 1 \\ -\delta_R & 0 \end{bmatrix}, \quad b = \begin{bmatrix} 1 \\ 0 \end{bmatrix}, \quad (2.2)$$

and $x = (x_1, x_2) \in \mathbb{R}^2$. Here $\tau_L, \delta_L, \tau_R, \delta_R \in \mathbb{R}$ are parameters; the BCB parameter, usually denoted μ , has been scaled to 1.

The dynamics and bifurcation structure of (2.1)–(2.2) is incredibly rich [2, 35, 19]. It exhibits robust chaos [3] in the sense that chaotic attractors exist throughout open regions of (four-dimensional) parameter space, even with $\delta_L \delta_R > 0$ where the map is invertible. Fig. 1 shows a phase portrait of such an attractor. The attractor contains a saddle fixed point, and, remarkably, its stable manifold is dense in an open region of phase space. This was proved in [16] via a series of geometric arguments by bounding the rate at which line segments expand. A similar result was obtained earlier by Misiurewicz [27] for the Lozi family (the special case $\tau_L = -\tau_R$ and $\delta_L = \delta_R$). Despite being one-dimensional, the stable manifold densely fills a

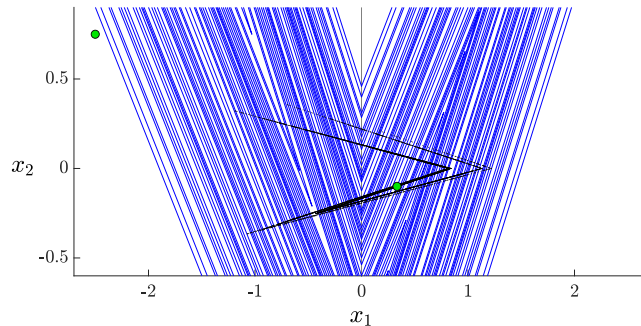


Figure 1: A phase portrait of an invertible instance of the two-dimensional BCNF (2.1)–(2.2); specifically $(\tau_L, \delta_L, \tau_R, \delta_R) = (1.7, 0.3, -1.7, 0.3)$. In black we show 8000 consecutive iterates of a typical forward orbit with transients removed (this represents the attractor of the map). The green circles are fixed points; the blue lines show the stable manifold (grown outwards numerically some amount) of the right-most fixed point.

two-dimensional region, so in this sense is a blender. Hence for two-dimensional, invertible maps, blenders are possible if the map is C^0 but not C^1 .

3 Transition through unstable dimension variability

The parameter space of the two-dimensional BCNF has regions where the map has a chaotic attractor in which (the dense set of) periodic solutions are all saddles, and other regions where the map has a chaotic attractor in which periodic solutions are all repellers. In this section we interpolate between two such regions and provide numerical evidence for robust UDV.

Let $x \in \mathbb{R}^2$ be a period- n point of (2.1)–(2.2) and suppose its forward orbit does not intersect the switching manifold (as is generically the case). In a neighbourhood of the orbit the map is differentiable (in fact affine). Thus it has two stability multipliers, and if neither of these has modulus 1, the orbit is hyperbolic. In this case let $k \in \{0, 1, 2\}$ denote the number of stability multipliers with modulus greater than 1. Then x is asymptotically stable if $k = 0$, a saddle if $k = 1$, and a repeller if $k = 2$.

We now explore a one-parameter family of examples. In (2.2) we use

$$\begin{aligned}
 \tau_L &= (1 - a)\tau_{L,0} + a\tau_{L,1}, \\
 \delta_L &= (1 - a)\delta_{L,0} + a\delta_{L,1}, \\
 \tau_R &= (1 - a)\tau_{R,0} + a\tau_{R,1}, \\
 \delta_R &= (1 - a)\delta_{R,0} + a\delta_{R,1},
 \end{aligned} \tag{3.3}$$

with $0 \leq a \leq 1$ and

$$\begin{aligned}
\tau_{L,0} &= 0.8, & \tau_{L,1} &= 0.8, \\
\delta_{L,0} &= -0.8, & \delta_{L,1} &= -1.2, \\
\tau_{R,0} &= -2.8, & \tau_{R,1} &= -1, \\
\delta_{R,0} &= 0.8, & \delta_{R,1} &= 2.4.
\end{aligned}
\tag{3.4}$$

This one-parameter family has been chosen for three reasons. First, with $a = 0$ all periodic solutions are saddles, Fig. 2-a. This is because with $|\delta_L|, |\delta_R| < 1$ both pieces of (2.1) are area-contracting so repellers are not possible, while stable periodic solutions are not possible because an invariant expanding cone can be constructed in tangent space [21]. Second, with $a = 1$ all periodic solutions, except the left-most fixed point, appear to be repellers, Fig. 2-c. This has been proved for nearby parameter combinations where there exists a simple Markov partition [20, 18]. Third, the map appears to have a unique attractor for all $0 \leq a \leq 1$. The two Lyapunov exponents of the attractor are shown in Fig. 3. These were computed numerically using the standard QR-factorisation method [15, 39].

For any $0 \leq a \leq 1$, let $\mathcal{N}(k, n; a)$ denote the number of period- n points that have k stability multipliers with modulus greater than 1. The sum of these numbers up to $n = 25$ is plotted in Fig. 4-a. This figure was computed by brute-force. We used Duval’s algorithm [14] to generate all sequences of L ’s and R ’s of length $n \leq 25$. Interpreting these as applications of (2.1) on the left or on the right respectively, the (generically) unique point that has period n in the order specified by each sequence was identified for each value of a [32]. We then checked by iterating the map whether the order of the images of the point matched the order of the specified sequence (an *admissibility* condition). For those admissible sequences the stability multipliers were evaluated to determine whether the periodic solution is a saddle or

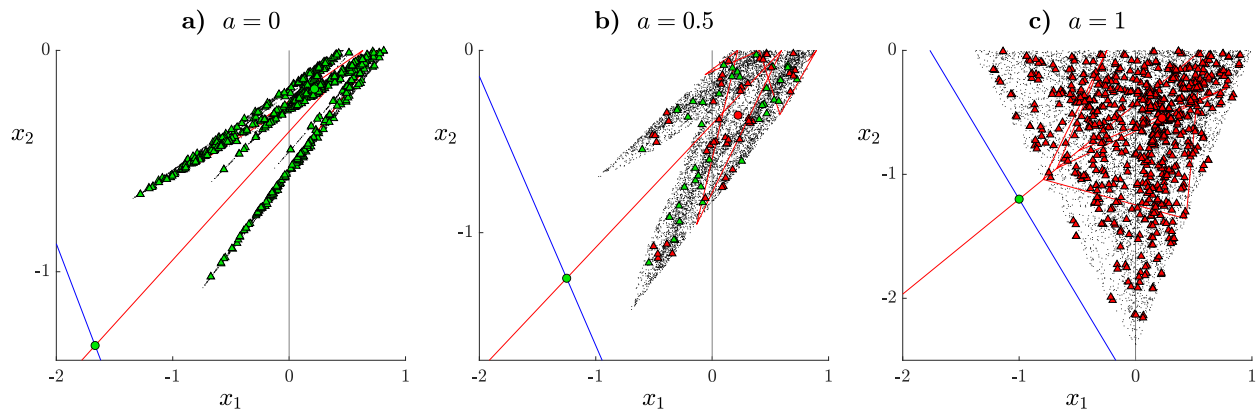


Figure 2: Phase portraits of non-invertible instances of the two-dimensional BCNF (2.1)–(2.2). The parameter values are given by (3.3) with (3.4) and three different values of a . The black dots show iterates of a typical forward orbit with transients removed. Periodic points (up to period 10) are shown with triangles, except fixed points are shown with circles. Saddles are coloured green; repellers are coloured red. The stable (blue) and unstable (red) manifolds of the left-most fixed point are also shown (grown outwards a small amount).

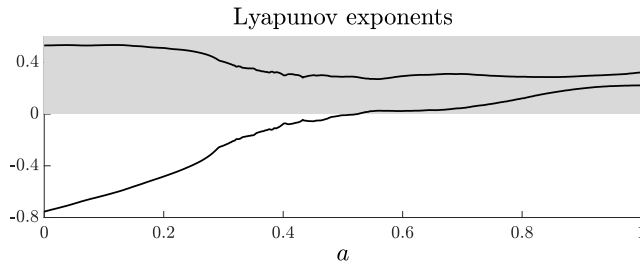


Figure 3: Numerically computed Lyapunov exponents of the attractor of (2.1)–(2.2) with (3.3) and (3.4).

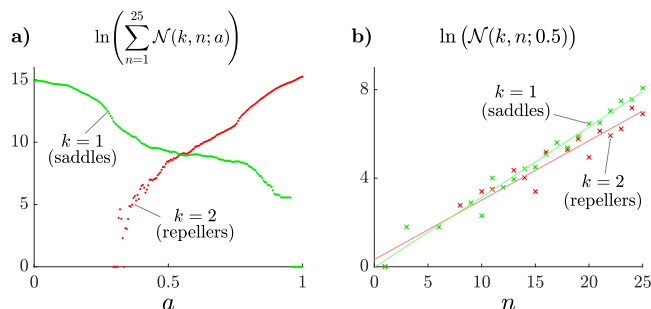


Figure 4: Plots involving $\mathcal{N}(k, n; a)$: the number of period- n points (saddles for $k = 1$; repellers for $k = 2$) of (2.1)–(2.2) with (3.3) and (3.4). Panel (b) includes lines of best fit.

a repeller.

For an intermediate range of values of a , the attractor contains both saddles and repellers, thus exhibits UDV. The point of cross-over, where saddles and repellers exist in the same proportion, is close to $a = 0.5$ and matches well to where the lower Lyapunov exponent becomes positive. Fig. 2-b shows a phase portrait with $a = 0.5$; Fig. 4-b shows that here the number of saddles and repellers appears to increase exponentially with n . This suggests that saddles and repellers are both dense in the attractor.

Saddles and repellers can arise in different ways. As the value of a is decreased from 1, saddles appear to be first created in a BCB of period-five solutions at $a \approx 0.9592$. Here infinitely many saddle periodic points are created because the BCB also creates robust heteroclinic connections between two saddle period-five solutions. This explains the large discontinuity in the number of saddle points in Fig. 4-a. In contrast, as the value of a is increased from 0, repellers are created and destroyed in many bifurcations. For example a saddle period-nine solution (with only one point in $x_1 < 0$) becomes repelling at $a \approx 0.3278$ when one of its stability multipliers decreases through -1 , then is destroyed in a BCB at $a \approx 0.3321$.

Since the maps are non-invertible, repelling sets may have preimages, i.e. they may have zero dimensional stable manifolds leading to phenomena such as snap-back repellers [17]. We conjecture that the saddle chaotic set associated with the period-five heteroclinic cycle at $a \approx 0.9592$ provides the larger set required to give robust intersections between its one-

dimensional unstable manifold and the zero-dimensional stable manifolds of the repellers as a decreases further, thus creating the conditions for blenders to exist. The transition at lower values of a to the appearance of repellers is less clear. It may be that ‘enough’ repellers need to be created before a persistent connection between their zero-dimensional stable manifolds and the unstable manifolds of the saddles can be created.

4 An explicit heterodimensional cycle

We now provide a simple example of a heterodimensional cycle. Fig. 5 shows a phase portrait of (2.1) with

$$\tau_L \approx 0.8716, \quad \delta_L = -1, \quad \tau_R = -1.5, \quad \delta_R = 2, \quad (4.5)$$

where the exact value of τ_L will be clarified in a moment. With these values the right-most fixed point (red circle), call it x^R , is repelling. There also exists a saddle period-three solution (green triangles). The value of τ_L has been chosen so that the unstable manifold of the period-three solution intersects x^R . By using computer algebra to analytically find where a certain fourth preimage of x^R lies on the initial linear part of the unstable manifold, we found that τ_L is a root of

$$108\tau_L^6 + 495\tau_L^5 + 258\tau_L^4 + 1184\tau_L^3 - 5800\tau_L^2 - 4907\tau_L + 7454. \quad (4.6)$$

The (two-dimensional) unstable manifold of x^R appears to intersect the stable manifold of the period-three solution (as one would expect), thus these orbits have a heteroclinic

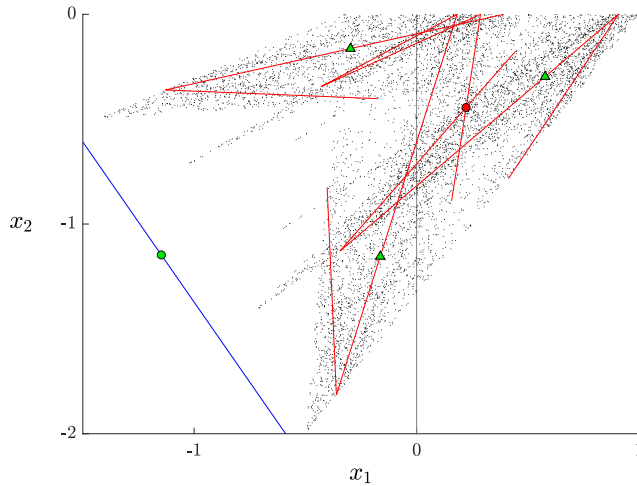


Figure 5: A phase portrait of a non-invertible instance of the two-dimensional BCNF, (2.1)–(2.2) with (4.5). The black dots show iterates of a typical forward orbit with transients removed. The blue line is the initial part of the stable manifold of the left-most fixed point (green circle). The red lines show part of the unstable manifold of a period-three solution (green triangles). The value of τ_L has been chosen so that this manifold intersects the right-most fixed point (red circle).

connection. This is a heterodimensional cycle because x^R and the period-three solution have unstable manifolds of different dimensions. This cycle is codimension-one because their dimensions differ by one; indeed the cycle was obtained by carefully adjusting the value of one parameter (namely τ_L).

Fig. 5 is the simplest example of a heterodimensional cycle that we have found for (2.1)–(2.2) where the cycle is contained in an attractor. This suggests that, as in Fig. 2-b, the attractor exhibits UDV.

5 Unstable dimension variability in invertible maps

For an invertible map to have a heterodimensional cycle, the map needs to be at least three dimensional. This can also be demonstrated with the BCNF. In three dimensions the BCNF is (2.1) with

$$A_L = \begin{bmatrix} \tau_L & 1 & 0 \\ -\sigma_L & 0 & 1 \\ \delta_L & 0 & 0 \end{bmatrix}, \quad A_R = \begin{bmatrix} \tau_R & 1 & 0 \\ -\sigma_R & 0 & 1 \\ \delta_R & 0 & 0 \end{bmatrix}, \quad b = \begin{bmatrix} 1 \\ 0 \\ 0 \end{bmatrix}, \quad (5.7)$$

and $x = (x_1, x_2, x_3) \in \mathbb{R}^3$, and has been studied previously for instance in [10, 33].

Fig. 6 shows a phase portrait using

$$\begin{aligned} \tau_L &= 0.7228540306, & \sigma_L &= -1, & \delta_L &= -0.2, \\ \tau_R &= -1.5, & \sigma_R &= 2, & \delta_R &= -0.2. \end{aligned} \quad (5.8)$$

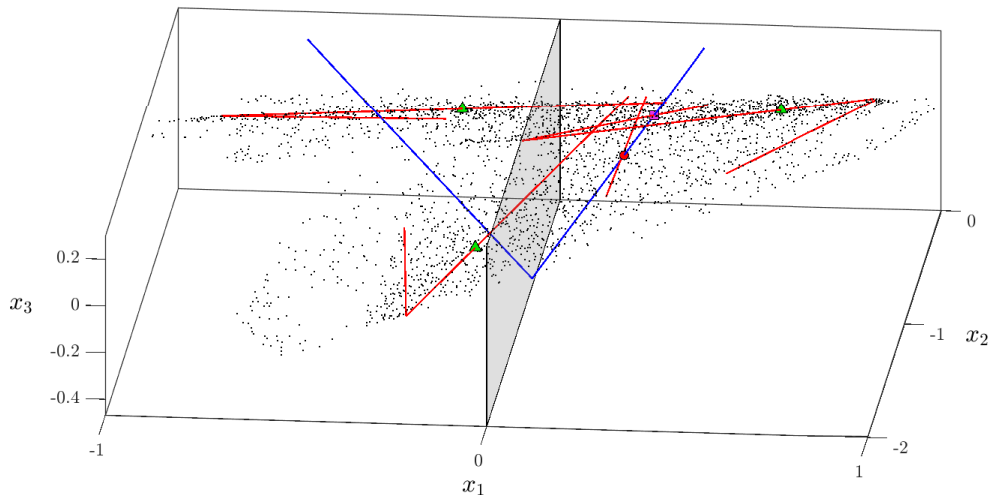


Figure 6: A phase portrait of an invertible instance of the three-dimensional BCNF, (2.1) with (5.7) and (5.8). The black dots show iterates of a typical forward orbit with transients removed. The one-dimensional stable manifold of a fixed point (red circle) approximately intersects the one-dimensional unstable manifold of a period-three solution (green triangles). One point of intersection is indicated with a pink square.

These values were obtained by adding a dimension to the example of Fig. 5, varying δ_L and δ_R from 0 to create fully three-dimensional dynamics, and lastly adjusting the value of τ_L (to 10 decimal places) so that the one-dimensional unstable manifold of the period-three solution approximately intersects the one-dimensional stable manifold of x^R . The pink square in Fig. 6 shows this approximate point of intersection. Since the invariant manifolds appear to be embedded in an attractor, the other invariant manifolds presumably intersect forming a heterodimensional cycle. Hence this attractor too has UDV.

Numerically we grown the unstable manifold of the period-three solution outwards much further than that shown in Fig. 6. Fig. 7 shows the intersections of this manifold with the switching manifold $x_1 = 0$. The intersections have a quasi-one-dimensional structure suggesting that the unstable manifold is essentially two-dimensional, so a blender.

6 Discussion

The existence of UDV due to blenders has been established numerically in three-dimensional generalisations of the Hénon map [30, 31]. We have considered a related piecewise-linear family and by interpolating between parameters with only saddles and parameters with only repellers we have provided strong numerical evidence for the existence of UDV in the two-dimensional non-invertible BCNF and the three-dimensional invertible BCNF. Since the BCNF describes BCBs in general piecewise-smooth systems the existence of UDV in these examples shows that UDV has broader significance within the study of piecewise-smooth dynamical systems and their applications.

We have also identified a possible mechanism for the onset of UDV through the creation of saddle chaotic sets (as the parameter a in Fig. 4 decreases) and snap-back repellers (as a increases). These may provide stable and unstable manifolds of the appropriate dimensions to create blenders with the infinite families of periodic orbits (either repellers or saddles) that already exist. This conjectural connection merits further study, with comparisons to the bifurcation theory approaches of [1, 4].

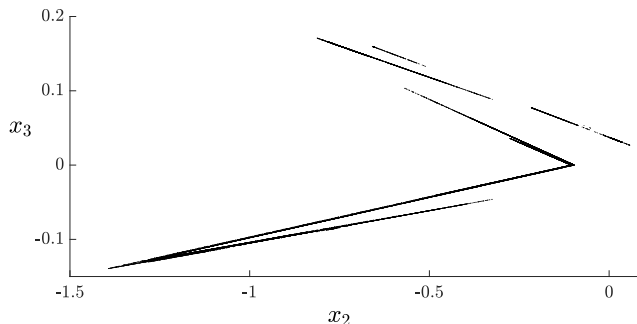


Figure 7: Intersections of the one-dimensional unstable manifold of the period-three solution of Fig. 6 with $x_1 = 0$. This was computed by growing the manifold much further than that shown in Fig. 6.

Acknowledgements

The authors were supported by Marsden Fund contract MAU1809, managed by Royal Society Te Apārangi.

References

- [1] K.T. Alligood, E. Sander, and J.A. Yorke. Crossing bifurcations and unstable dimension variability. *Phys. Rev. Lett.*, 96:244103, 2006.
- [2] S. Banerjee and C. Grebogi. Border collision bifurcations in two-dimensional piecewise smooth maps. *Phys. Rev. E*, 59(4):4052–4061, 1999.
- [3] S. Banerjee, J.A. Yorke, and C. Grebogi. Robust chaos. *Phys. Rev. Lett.*, 80(14):3049–3052, 1998.
- [4] E. Barreto and P. So. Mechanisms for the development of unstable dimension variability and the breakdown of shadowing in coupled chaotic systems. *Phys. Rev. Lett.*, 85(12):2490–2493, 2000.
- [5] C. Bonatti and L.J. Díaz. Robust heterodimensional cycles and C^1 -generic dynamics. *J. Inst. Math. Jussieu*, 7:469–525, 2008.
- [6] C. Bonatti, L.J. Díaz, and S. Kiriki. Stabilization of heterodimensional cycles. *Nonlinearity*, 25:931–960, 2012.
- [7] C. Bonatti, L.J. Díaz, and M. Viana. *Dynamics Beyond Uniform Hyperbolicity*. Springer, New York, 2005.
- [8] S. Das and J.A. Yorke. Multichaos from quasiperiodicity. *SIAM J. Appl. Dyn. Syst.*, 16(4), 2017.
- [9] S. Dawson, C. Grebogi, T. Sauer, and J.A. Yorke. Obstructions to shadowing when a Lyapunov exponent fluctuates about zero. *Phys. Rev. Lett.*, 73(14):1927–1930, 1994.
- [10] S. De, P.S. Dutta, S. Banerjee, and A.R. Roy. Local and global bifurcations in three-dimensional, continuous, piecewise-smooth maps. *Int. J. Bifurcation Chaos*, 21(6):1617–1636, 2011.
- [11] M. di Bernardo. Normal forms of border collision in high dimensional non-smooth maps. In *Proceedings IEEE ISCAS, Bangkok, Thailand*, volume 3, pages 76–79, 2003.
- [12] M. di Bernardo, P. Kowalczyk, and A. Nordmark. Sliding bifurcations: A novel mechanism for the sudden onset of chaos in dry friction oscillators. *Int. J. Bifurcation Chaos*, 13(10):2935–2948, 2003.
- [13] Y. Do and Y.-C. Lai. Statistics of shadowing time in nonhyperbolic chaotic systems with unstable dimension variability. *Phys. Rev. E*, 69:016213, 2004.

- [14] J.-P. Duval. Génération d’une section des classes de conjugaison et arbre des mots de Lyndon de longueur bornée. *Theoret. Comput. Sci.*, 60:255–283, 1988. In French.
- [15] J.-P. Eckmann and D. Ruelle. Ergodic theory of chaos and strange attractors. *Rev. Mod. Phys.*, 57(3):617–656, 1985.
- [16] I. Ghosh and D.J.W. Simpson. Robust Devaney chaos in the two-dimensional border-collision normal form. *Chaos*, 32:043120, 2022.
- [17] P. Glendinning. Bifurcations of snap-back repellers with application to border-collision bifurcations. *Int. J. Bifurcation Chaos*, 20:479–489, 2010.
- [18] P. Glendinning. Bifurcation from stable fixed point to 2D attractor in the border collision normal form. *IMA J. Appl. Math.*, 81(4):699–710, 2016.
- [19] P. Glendinning and D.J.W. Simpson. Chaos in the border-collision normal form: A computer-assisted proof using induced maps and invariant expanding cones. *Appl. Math. Comput.*, 434:127357, 2022.
- [20] P. Glendinning and C.H. Wong. Two dimensional attractors in the border collision normal form. *Nonlinearity*, 24:995–1010, 2011.
- [21] P.A. Glendinning and D.J.W. Simpson. A constructive approach to robust chaos using invariant manifolds and expanding cones. *Discrete Contin. Dyn. Syst.*, 41(7):3367–3387, 2021.
- [22] A. Hammerlindl, B. Krauskopf, G. Mason, and H.M. Osinga. Determining the global manifold structure of a continuous-time heterodimensional cycle. To appear: *J. Comput. Dyn.*, 2022.
- [23] S. Hittmeyer, B. Krauskopf, H.M. Osinga, and K. Shinohara. Existence of blenders in a Hénon-like family: geometric insights from invariant manifold computations. *Nonlinearity*, 31(10):R239–R267, 2018.
- [24] S. Hittmeyer, B. Krauskopf, H.M. Osinga, and K. Shinohara. How to identify a hyperbolic set as a blender. *Discrete Cont. Dyn. Syst.*, 40(12):6815–6836, 2020.
- [25] E.J. Kostelich, I. Kan, C. Grebogi, E. Ott, and J.A. Yorke. Unstable dimension variability: A source of nonhyperbolicity in chaotic systems. *Phys. D*, 109:81–90, 1997.
- [26] Y.-C. Lai and C. Grebogi. Modeling of coupled chaotic oscillators. *Phys. Rev. Lett.*, 82(24):4803–4806, 1999.
- [27] M. Misiurewicz. Strange attractors for the Lozi mappings. In R.G. Helleman, editor, *Nonlinear dynamics, Annals of the New York Academy of Sciences*, pages 348–358, New York, 1980. Wiley.
- [28] H.E. Nusse and J.A. Yorke. Border-collision bifurcations including “period two to period three” for piecewise smooth systems. *Phys. D*, 57:39–57, 1992.

- [29] T. Puu and I. Sushko, editors. *Business Cycle Dynamics: Models and Tools*. Springer-Verlag, New York, 2006.
- [30] Y. Saiki, M.A.F. Sanjuán, and J.A. Yorke. Low-dimensional paradigms for high-dimensional hetero-chaos. *Chaos*, 28(10):103110, 2018.
- [31] Y. Saiki, H. Takahasi, and J.A. Yorke. Piecewise-linear maps with heterogeneous chaos. *Nonlinearity*, 34:5744–5761, 2021.
- [32] D.J.W. Simpson. Border-collision bifurcations in \mathbb{R}^n . *SIAM Rev.*, 58(2):177–226, 2016.
- [33] D.J.W. Simpson. Grazing-sliding bifurcations creating infinitely many attractors. *Int. J. Bifurcation Chaos*, 27(12):1730042, 2017.
- [34] D.J.W. Simpson and P.A. Glendinning. Inclusion of higher-order terms in the border-collision normal form: persistence of chaos and applications to power converters. Submitted to: *Phys. D*. [arXiv:2111.12222](https://arxiv.org/abs/2111.12222), 2021.
- [35] D.J.W. Simpson and J.D. Meiss. Neimark-Sacker bifurcations in planar, piecewise-smooth, continuous maps. *SIAM J. Appl. Dyn. Sys.*, 7(3):795–824, 2008.
- [36] R. Szalai and H.M. Osinga. Arnol’d tongues arising from a grazing-sliding bifurcation. *SIAM J. Appl. Dyn. Sys.*, 8(4):1434–1461, 2009.
- [37] R.L. Viana, J.R.R. Barbosa, and C. Grebogi. Unstable dimension variability and codimension-one bifurcations of two-dimensional maps. *Phys. Lett. A*, 321:244–251, 2004.
- [38] R.L. Viana and C. Grebogi. Unstable dimension variability and synchronization of chaotic systems. *Phys. Rev. E*, 62(1):462–468, 2000.
- [39] H.F. von Bremen, F.E. Udawadia, and W. Proskurowski. An efficient QR based method for the computation of Lyapunov exponents. *Phys. D*, 101:1–16, 1997.
- [40] W. Zhang, B. Krauskopf, and V. Kirk. How to find a codimension-one heteroclinic cycle between two periodic orbits. *Discrete Contin. Dyn. Syst.*, 32(8):2825–2851, 2012.
- [41] Z.T. Zhusubaliyev, O.O. Yanochkina, E. Mosekilde, and S. Banerjee. Two-mode dynamics in pulse-modulated control systems. *Annual Rev. Control*, 34:62–70, 2010.